

Enhanced entanglement induced by Coulomb interaction in coupled optomechanical systems

Amjad Sohail¹ , Rizwan Ahmed², Chang Shui Yu³  and Tariq Munir¹

¹Department of Physics, Government College University Faisalabad, Allama Iqbal Road, 38000 Faisalabad, Pakistan

²Physics Division, Pakistan Institute of Nuclear Science and Technology (PINSTECH), PO Nilore, Islamabad 45650, Pakistan

³School of Physics, Dalian University of Technology, Dalian 116024, People's Republic of China

E-mail: amjadsohail@gcuf.edu.pk

Received 15 July 2019, revised 27 September 2019

Accepted for publication 15 October 2019

Published 5 February 2020



CrossMark

Abstract

We consider a coupled optomechanical system, in which two charged mechanical resonators are coupled through long range Coulomb interaction. It is shown that remote entanglement between the two charged mechanical resonators can be achieved by long range Coulomb interaction. Such a coupled optomechanical system exhibits the classical to quantum transition behavior. The outcome of our numerical simulation shows that in the absence of optomechanical coupling, quantum entanglement between the two mechanical resonators can be achieved for large Coulomb coupling strengths and small effective temperature. In addition, the entanglement between the two mechanical resonators can be enhanced through input laser power. We also investigate the entanglement transfer through Coulomb interaction and optomechanical couplings.

Keywords: entanglement, optomechanical system, Coulomb interaction

(Some figures may appear in colour only in the online journal)

1. Introduction

Quantum entanglement [1, 2], as a cornerstone of quantum physics, plays an important role in the foundation of quantum theory and also has many applications in quantum world, such as quantum metrology [3] and quantum information science [4]. In particular, how to prepare macroscopic mechanical entanglement is of high interest and significance because such macroscopic entanglement might provide explicit proof for quantum phenomena [5] and might potentially help us to elucidate the quantum to classical transition [6, 7]. So far, one has had a fairly good understanding of how to generate entanglement among microscopic entities. Moreover, the entanglement has been successfully prepared and manipulated in many microscopic systems, such as atoms [8–12], photons [13–15], ions [16–19] Bose–Einstein condensates [20, 21], and so on.

Recently, the research of micro-mechanical resonators (MRs) has attracted considerable interests in both nano-technology and quantum mechanics in the past decade, because of the fact that micro-mechanical resonators is an ideal candidate to search quantum properties. These quantum properties not only provide insights into the fundamental physical principle in quantum regime [22], but also give many applications of MRs, such as, quantum information processing [23, 24], optomechanical metrology [25], gravitational wave detection [26] and biological sensing [27]. However, only few quantum properties on MRs can be obtained experimentally directly, since the quantum properties on MRs are very much difficult to observe. Therefore, it is desirable to observe more quantum properties on MRs. The steady entanglement between the MRs is one of this type of quantum properties.

Until now, numerous schemes have been proposed to establish entanglement between the micro-mechanical

resonators from different angles of view: such as entangling two remotely separated resonators by employing the entangled light fields [28], realizing entanglement between two dielectric membranes [29] and establishing entanglement between two micro-mechanical resonators induced by the radiation pressure in a two-cavity optomechanical system [30]. Particularly, long range entanglement between two micro-mechanical resonators in separated cavities via injecting squeezed light or conditional quantum measurements is examined [28, 31, 32]. Also, it was revealed that weak mechanical entanglement between two distant resonators can be obtained simply by optomechanical coupling [33]. The remote entanglement of distant elements is of great importance for establishing long-distance quantum communication networks [34, 35].

In an interesting study by Chen *et al* Coulomb assisted optomechanical setup has been considered [36]. They have discussed dissipation induced optomechanical entanglement and found that there is a considerable dependence of entanglement on the Coulomb interaction strength. In their scheme, they have a single optical mode coupled with a mechanical resonator which further is coupled to a second mechanical resonator through a Coulomb force. Bai *et al* considered a similar optomechanical system with an additional contribution due to the inclusion of a degenerate OPA [37], which provides some additional features such as entanglement enhancement, since OPA leads to squeezed optical field. In another interesting study, Bai *et al* [38] have presented a scheme for robust entanglement in an optomechanical system consisting of two coupled optomechanical cavities. In their study, they considered the coherently driven ensemble of two-level atoms inside one of the cavity. Their results show that enhancement of entanglement is strongly dependent on the optomechanical coupling strength.

In our present study, we have considered a different scheme than their schemes. Here, we have considered two independent optomechanical cavity systems having two mechanical resonators which are mutually coupled through Coulomb force. These mechanical elements are spatially separated by a distance r . We throughout the study focused the effects of Coulomb coupling upon the entanglement. An interesting result of our study is that Coulomb interaction implies a finite non-zero entanglement even at zero effective optomechanical coupling. Our results show that increased Coulomb coupling strength improves the degree of entanglement. Furthermore, we propose a coupled optomechanical system to create the distant entanglement between two micro-mechanical resonators due to long rang Coulomb interaction exhibiting the classical to quantum transition behavior. Our scheme that the entanglement between the two mechanical resonators by Coulomb interaction is different from the conventional optomechanical system which the entanglement between two movable mechanical resonators is induced by the external atoms [39] or bring forth by the inner cavity modes [40]. Contrast to previously conventional methods, the Coulomb interaction between the two micro-mechanical resonators belongs to long-range interactions [36, 41, 42]. Furthermore, we also show the enhancement of the

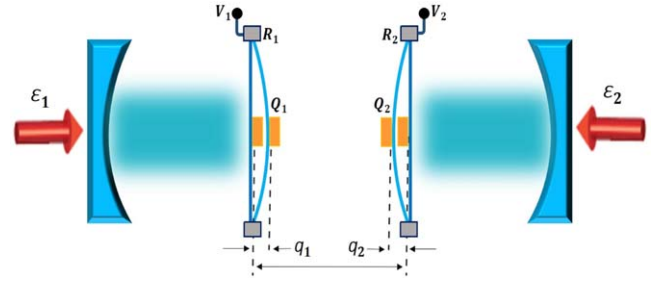


Figure 1. Schematic diagram of 2 coupled OMS. The left and right cavity comprise a fixed mirror and a mechanical resonators R_1 (R_2). The two mirrors coupled to each other under the action of the Coulomb interaction. The electrode having charge Q_1 (Q_2) on R_1 (R_2) is charged by voltage V_1 (V_2). The equilibrium separation between R_1 and R_2 is r . The small deviation of R_1 and R_2 , due to Coulomb interaction and radiation pressure interaction, from their equilibrium positions are q_1 and q_2 respectively. The left (right) cavity is driven by a controlled field ε_1 (ε_2).

entanglement between the two micro-mechanical resonators through the input laser power. In addition, transferring entanglement between subsystem is very helpful to study the information storage in the quantum information processing [38, 43–46]. In the present work, we also show how the entanglement between the two mechanical resonators can be transferred to the entanglement between optical cavity field and the mechanical resonator either by decreasing the Coulomb coupling strength between the two mirrors or by increasing the input laser field.

This paper is organized as follows. In section 2, we introduce the optomechanical model, present the equations of motion, steady state values and linearized quantum Langevin equations. In section 3, we transform the quantum Langevin equations into a equivalent differential equation of the covariance matrix. In section 4, we present the numerical results and quantify the entanglement measurement of the two charged mechanical resonators using logarithmic negativity and the section 5 concludes our paper.

2. The model and the dynamics

The system under consideration comprises two spatially separated optomechanical cavities. The two partially transmitting mirrors, at a distance r , are in contact with a thermal bath in equilibrium at temperature T . As shown schematically in figure 1, the two movable mechanical resonators of the two cavities are coupled through the long rang Coulomb interactions Γ . The two optomechanical cavities are separately driven by a coupling field with amplitudes $\varepsilon_j = \sqrt{\frac{2\kappa_j \wp_j}{\hbar\omega_L}}$ where κ_j and \wp_j are the decay rate and the pump power corresponding to the j th cavity field. We describe the optical modes of the two cavities, respectively, by annihilation (creation) operators c_j (c_j^\dagger) where $j = 1, 2$. The momentum and position operators of the mechanical resonators are represented by p_j and q_j where $j = 1, 2$. The optomechanical coupling strength between the optical field and the mechanical resonator is

given by $g_j = \frac{\hbar\omega_c}{L} \sqrt{\frac{\hbar}{m_j\omega_m}}$ where L is the length of each cavity.

The similar description can be found in [47]. The Hamiltonian of the coupled optomechanical system is given by

$$H = \sum_{j=1,2} \hbar \left[\omega_c c_j^\dagger c_j + \frac{\omega_j}{2} (p_j^2 + q_j^2) - g_j c_j^\dagger c_j q_j \right] + \sum_{j=1,2} i\hbar (c_j^\dagger \varepsilon_j e^{-i\omega_L t} - c_j \varepsilon_j^* e^{i\omega_L t}) + H_{\text{CI}}, \quad (1)$$

where the first term in square bracket is the free Hamiltonian for a two single mode cavities, second term describes the vibration of the two charged resonators and third term corresponds to respective cavity-mechanical resonator interaction. The first term in the second line represents the interaction of optomechanical cavities and the external laser fields. The second term in the second line represents the Coulomb interaction between two charged resonators R_1 and R_2 is given as $H_{\text{CI}} = \frac{-C_1 V_1 C_2 V_2}{4\pi\epsilon_0 |r + q_1 - q_2|}$ with r being the equilibrium separation between two resonators. The two resonators R_1 and R_2 take the charges $Q_1 = C_1 V_1$ and $Q_2 = -C_2 V_2$ with $C_1(C_2)$ and $V_1(-V_2)$ being the capacitance and the voltage of the bias gate, respectively. We assume the distance between the two charged resonators is much greater than the small oscillations of the charged resonators $r \gg q_i$, the term describing the interaction between two charged resonators can be expanded to the second order as:

$$H_{\text{CI}} = \frac{-C_1 V_1 C_2 V_2}{4\pi\epsilon_0 r} \left[1 - \frac{q_1 - q_2}{r} + \frac{(q_1 - q_2)^2}{r^2} \right]. \quad (2)$$

The linear term can be absorbed into the definition of the equilibrium positions, and the quadratic term includes a re-normalization of the oscillation frequency for both resonators R_1 and R_2 . Through further omitting the constant term, the Coulomb interaction term can be written in a simpler form

$$H_{\text{CI}} = \hbar\Gamma q_1 q_2, \quad (3)$$

where $\Gamma = \frac{C_1 V_1 C_2 V_2}{4\pi\epsilon_0 m\omega_m r^3}$ [36, 48–50]. In the rotating frame at the coupling frequency ω_L , the Hamiltonian of our system can be written as

$$H = \sum_{j=1,2} \hbar \left[\delta_j c_j^\dagger c_j + \frac{\omega_j}{2} (p_j^2 + q_j^2) - g_j c_j^\dagger c_j q_j \right] + \hbar\Gamma q_1 q_2 + \sum_{j=1,2} i\hbar (\varepsilon_j c_j^\dagger - \varepsilon_j^* c_j), \quad (4)$$

where $\delta_j = \omega_c - \omega_L$. The set of nonlinear Langevin equations for this system can be written as

$$\begin{aligned} \dot{q}_j &= \omega_j p_j, \\ \dot{p}_j &= -\omega_j q_j - \Gamma q_k + g_j c_j^\dagger c_j - \gamma_j p_j + \xi_j, \quad j \neq k \\ \dot{c}_j &= -(\kappa_j + i\delta_j) c_j + ig_j c_j q_j + \varepsilon_j + \sqrt{2\kappa_j} c_{\text{in}}^j, \end{aligned} \quad (5)$$

where κ_j is the decay rate of the cavities and γ_j is the damping rate of mechanical resonators.

We now begin to linearize the dynamics of the coupled optomechanical system. The nonlinear quantum Langevin equations can be linearized by rewriting each Heisenberg operator as a sum of its steady-state mean value and an

additional fluctuation operator, i.e.

$$q_j = \bar{q}_j + \delta q_j, \quad p_j = \bar{p}_j + \delta p_j, \quad c_j = \bar{c}_j + \delta c_j, \quad j = 1, 2. \quad (6)$$

After inserting these expressions into the Langevin equations of equation (5), we can obtain a set of nonlinear algebraic equations for the steady state values and a set of quantum Langevin equations for the fluctuation operators. Through setting all the time derivatives in algebra equations for the steady state value to zero, the steady state mean values of coupled optomechanical system are given by,

$$\begin{aligned} \bar{q}_{j,0} &= \frac{\omega_k g_j |c_{j,0}|^2 - \Gamma g_k |c_{k,0}|^2}{\omega_j \omega_k - \Gamma^2}, \quad j \neq k \\ \bar{c}_{j,0} &= \frac{\varepsilon_j}{\kappa_j + i\Delta_j}, \end{aligned} \quad (7)$$

and the linearized Langevin equations

$$\begin{aligned} \delta \dot{q}_j &= \omega_j \delta p_j, \\ \delta \dot{p}_j &= -\omega_j \delta q_j - \Gamma \delta q_k + G_j (\delta c_j + \delta c_j^\dagger) - \gamma_j \delta p_j + \xi_j, \\ \delta \dot{c}_j &= -(\kappa_j + i\Delta_j) \delta c_j + iG_j \delta q_j + \sqrt{2\kappa_j} c_{\text{in}}^j, \end{aligned} \quad (8)$$

where $\Delta_j = \delta_j - g_j q_{j,0}$ are the effective optomechanical detunings and $G_j = g_j c_{j,0}$ represents the effective optomechanical coupling constants which is controlled by the cavity driving input power $\wp_1 = \wp_2 = \wp$.

3. Entanglement measurement of the two charged mechanical resonators

In this section, we adopt the standard nomenclature to find out the steady state entanglement [51]. We start looking into the measurement of the steady state entanglement between two charged mechanical resonators. Defining the quadratures $\delta X_j = \frac{1}{\sqrt{2}}(\delta c_j + \delta c_j^\dagger)$, $\delta Y_j = \frac{1}{\sqrt{2}i}(\delta c_j - \delta c_j^\dagger)$ and the corresponding Hermitian input noise operators $\delta X_{j,\text{in}} = \frac{1}{\sqrt{2}}(\delta c_{j,\text{in}} + \delta c_{j,\text{in}}^\dagger)$, $\delta Y_{j,\text{in}} = \frac{1}{\sqrt{2}i}(\delta c_{j,\text{in}} - \delta c_{j,\text{in}}^\dagger)$. Inserting the quadratures into equation (8) and separating of the imaginary and real part of equations we obtain:

$$\begin{aligned} \delta \dot{q}_j &= \omega_j \delta p_j, \\ \delta \dot{p}_j &= -\omega_j \delta q_j - \Gamma \delta q_k + G_j \delta X_j - \gamma_j \delta p_j + \xi_j, \\ \delta \dot{X}_j &= -\kappa_j \delta X_j + \Delta_j \delta Y_j + \sqrt{2\kappa_j} \delta X_{j,\text{in}}, \\ \delta \dot{Y}_j &= -\Delta_j \delta X_j - \kappa_j \delta Y_j + G_j \delta q_j + \sqrt{2\kappa_j} \delta Y_{j,\text{in}}. \end{aligned} \quad (9)$$

Finally we rewrite the Langevin equation in compact form as follow

$$\dot{F} = AF + \Xi, \quad (10)$$

where $F = (\delta X_1, \delta Y_1, \delta X_2, \delta Y_2, \delta q_1, \delta p_1, \delta q_2, \delta p_2)^T$ and $\Xi = (\sqrt{2\kappa_1}(X_1^{\text{in}}, Y_1^{\text{in}}), \sqrt{2\kappa_2}(X_2^{\text{in}}, Y_2^{\text{in}}), 0, \xi_1, 0, \xi_2)^T$ are the fluctuation and noise vectors respectively. The matrix A is

written as:

$$A = \begin{bmatrix} -\kappa_1 & \Delta_1 & 0 & 0 & 0 & 0 & 0 & 0 \\ -\Delta_1 & -\kappa_1 & 0 & 0 & G_1 & 0 & 0 & 0 \\ 0 & 0 & -\kappa_2 & \Delta_2 & 0 & 0 & 0 & 0 \\ 0 & 0 & -\Delta_2 & -\kappa_2 & 0 & 0 & G_2 & 0 \\ 0 & 0 & 0 & 0 & 0 & \omega_1 & 0 & 0 \\ G_1 & 0 & 0 & 0 & -\omega_1 & -\gamma_1 & -\Gamma & 0 \\ 0 & 0 & 0 & 0 & 0 & 0 & 0 & \omega_2 \\ 0 & 0 & G_2 & 0 & -\Gamma & 0 & -\omega_2 & -\gamma_2 \end{bmatrix}. \quad (11)$$

The coupled optomechanical system is stable and reaches its steady state only if the real part of all the eigenvalues of the matrix A have negative real parts. The stability conditions can be derived by applying the Routh–Hurwitz criterion. When the stability conditions of the coupled optomechanical system are satisfied, and the steady state Covariance matrix meets the following Lyapunov equation

$$AV + VA^T + D = 0, \quad (12)$$

where D is a diagonal matrix which is called diffusion matrix and characterizes the noise correlations

$$D = \text{diag}[\kappa_1, \kappa_1, \kappa_2, \kappa_2, 0, \gamma_1(2n_1 + 1), 0, \gamma_2(2n_2 + 1)]. \quad (13)$$

As, equation (13) is independent of frequency, we have the following Markovian approximation on the quantum Brownian noise

$$\frac{1}{2} \langle \hat{\xi}_i(t) \hat{\xi}_i(t') + \hat{\xi}_i(t') \hat{\xi}_i(t) \rangle \simeq \gamma_i(2n_i + 1) \delta(t - t'), \quad (14)$$

where n_i is the thermal phonon number and $i = 1, 2$. The Lyapunov equation (12) as a linear equation for V can be solved. Using the Simon condition for Gaussian states, we calculate the entanglement of the steady state [52–54]

$$E_N = \max[0, -2 \ln \eta^-], \quad (15)$$

where $\eta^- = 2^{-\frac{1}{2}} \sqrt{\sum [\varrho] - \sqrt{\sum [\varrho]^2 - 4 \det \varrho}}$ is the smallest symplectic eigenvalue of the partially transposed covariance matrix with

$$\varrho = \begin{pmatrix} \varrho_a & \varrho_c \\ \varrho_c^T & \varrho_b \end{pmatrix}, \quad (16)$$

and

$$\sum [\varrho] = \det \varrho_a + \det \varrho_b - 2 \det \varrho_c. \quad (17)$$

Here, ϱ_a , ϱ_b and ϱ_c are 2×2 block matrices.

4. Numerical results and discussions

In the following, we emphasize on the stationary dynamics of the system. Without loss of generality, we assume that all the parameters of the two mechanical resonators to be the same, i.e. $\omega_1 = \omega_2 = \omega_m$, $\gamma_1 = \gamma_2 = \gamma_m$. Similarly we also assume $\kappa_1 = \kappa_2 = \kappa$ and $\Delta_2 = \Delta_1 = \Delta$ for simplicity. In addition the input laser power from both sides is same i.e.

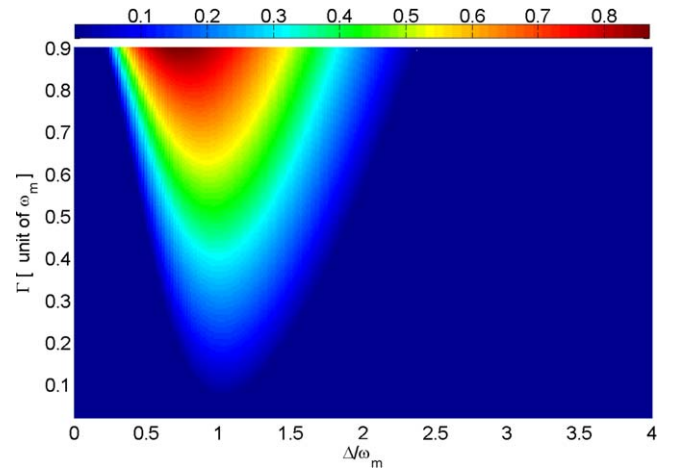


Figure 2. The logarithmic negativity E_N versus Δ/ω_m and Coulomb coupling strength Γ . The other parameters are $\omega_1 = \omega_2 = \omega_m = 2\pi \times 947$ kHz, $\gamma_1 = \gamma_2 = \gamma_m = 2\pi \times 141$ Hz, $\kappa_1 = \kappa_2 = \kappa = 2\pi \times 215$ kHz and $\wp_1 = \wp_2 = \wp = 4$ mW and $T = 10$ μ K.

$\wp_1 = \wp_2 = \wp$. We take the parameters from a recent experiment on the observation of the normal-mode splitting: [55] $\omega_m = 2\pi \times 947$ kHz, $\gamma_m = 2\pi \times 141$ Hz, $\kappa = 2\pi \times 215$ kHz, $m = 145$ ng, $\lambda = 1064$ nm and $L = 25$ mm. In addition, we have considered optical modes with zero occupancy.

During the last decade, there has been remarkable increase in experimental studies related to the practical aspects of optomechanical setups. These experiments are highly dependent on the availability of high- Q resonators [56–59]. In their seminal paper, Vitali *et al* gave a feasible experimental scheme for detection of mechanical motion [51]. There are many groups involved in the experimental setup for obtaining the macroscopic optomechanical entanglement. More recently, Riedinger and collaborators have experimentally demonstrated the remote entanglement between two micromechanical resonators which are 20 cm apart with high quality factor of $Q = 2.2 \times 10^5$ [60]. In another interesting experimental work, Marinkovic and collaborators have experimentally presented the optomechanical test for violation of Bell-type inequality [61]. In their experiment, Bell-type inequality violates for more than four-standard deviations, which shows the non-classical behavior of their system. Keeping these experimental studies, we have used the experimentally feasible system parameters. Therefore, our prediction presented in present paper, can be experimentally verified through similar kind of setups.

First, we explore the crucial role of Coulomb interaction on the entanglement between the two charged mechanical resonators separated in space. Figure 2 shows a density plot of E_N versus the normalized detuning Δ/ω_m and the Coulomb coupling strength at a temperature $T = 10$ μ K. As illustrated in previous section, as long as the logarithmic negativity $E_N > 0$, there is an entanglement between the mechanical resonators, meaning that there is a quantum correlation between two mechanical resonators, even though they are separated in space. With the increase of the coulomb coupling

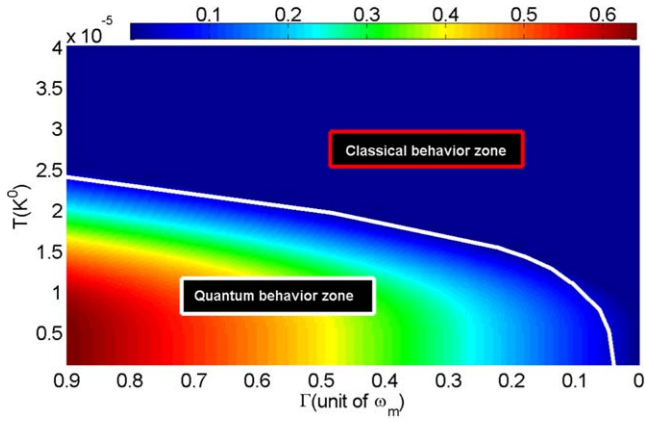


Figure 3. The logarithmic negativity E_N as a function of Coulomb coupling strength Γ/ω_m when $G_1 = G_2 = 0$ and the environment temperature T . The other parameters are same as in figure 2.

strength, not only the entanglement is progressively stronger but also the effective detuning's region that entanglement exists is more and more broader, which are very highly significant due to the fact that larger the value of the Coulomb coupling Γ , the stronger the mechanical resonators entangled, the broader the range of entanglement and consequently the more easily it is observed and realized in experiments. Our numerical results reveal that the maximum entanglement is almost linearly dependent on the strength of the Coulomb interaction around $\Delta/\omega_m = 1$. In addition, it is not possible to observe the entanglement between the two mechanical resonators if there is no Coulomb interaction. So the Coulomb interaction between the mechanical resonators is the essential reason of the entanglement. We can estimate the feasibility of the choice of numerical values of the Coulomb coupling strength Γ in recent experiment. If we adjust the gate voltage $V_1 = V_2 = 200$ V, the capacitance of the gate $C_1 = C_2 = 2.4$ nF and the separation between mechanical resonators without Coulomb and optomechanical interaction $r \simeq 160$ μm , in this situation $\Gamma \approx 0.4\omega_m$. If we compare the numerical values used in our coupled optomechanical system, it is obvious that our choice of numerical value of Coulomb coupling strength is easily executable in experiments.

In figure 3 we show how we switch from classical behavior to quantum behavior. For this purpose, we consider the important role of the optomechanical couplings G_1 and G_2 . Figure 3 shows a density plot of E_N versus the environment temperature T and the Coulomb coupling strength in the absence of the optomechanical couplings i.e. $G_1 = G_2 = 0$. As shown in figure 3, it can be seen that in the absence of optomechanical couplings, if we increase the Coulomb coupling and decrease the temperature, the system comprising two separated mechanical resonators in space will exhibit the quantum entanglement behavior. But as we increase the environment temperature, the thermal noise increases and as a result this quantum entanglement behavior will vanishes. From this result, we infer that an increase in temperature, leads to the transition from quantum to classical regime, which is obviously due to the thermal fluctuations. These thermal fluctuations are very important in a sense that they act

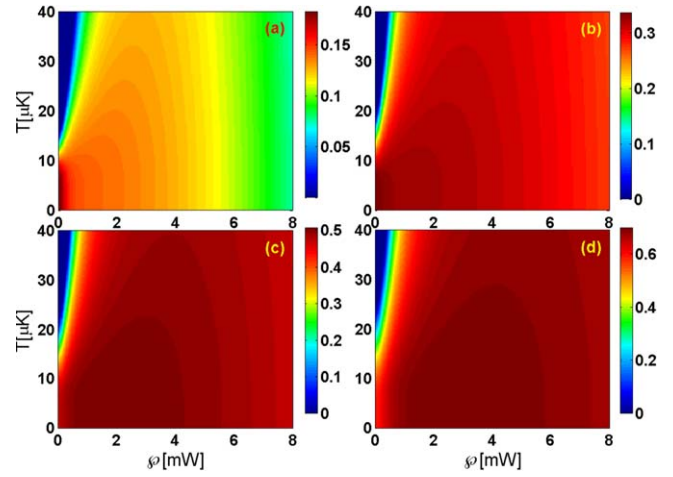


Figure 4. Plot of the logarithmic negativity E_N as a function of the environment temperature and input laser power for normalized detuning $\Delta/\omega_m = 1$ when (a) $\Gamma = 0.2\omega_m$, (b) $\Gamma = 0.4\omega_m$, (c) $\Gamma = 0.6\omega_m$ and (d) $\Gamma = 0.8\omega_m$. The other parameters are same as in figure 2.

as a Decoherence channel [6]. Hence, the system in classical regime do not shows any entanglement even though there exists quite strong Coulomb coupling strength. Due to this fact, we cannot observe the quantum behavior in macroscopic world. Hence the emergence of quantum behavior in macroscopic bodies in mechanical motion is usually bounded by the thermal noise. However, under the auxiliary of the two optomechanical couplings, the two mechanical resonators in the classical regime can exhibit the quantum entanglement and once the optomechanical couplings from both sides vanish, the entanglement between the mechanical resonators will vanish accordingly. Consequently, the system come back to the classical regime. This is because of the optomechanical couplings cool down the mechanical resonators and suppresses harmful effect of the thermal noise. Therefore, the optomechanical couplings play an important role to study the transition from classical behavior to quantum behavior.

Next, we examine the variation of the entanglement between the two mechanical resonators versus the input laser power and the temperature of the phonon reservoir. Figure 4 shows the steady-state entanglement between the two mechanical resonators, measured by the logarithmic negativity, E_N , as a function of the strength of laser power ϕ and the temperature of the phonon reservoir T for the normalized detuning $\Delta/\omega_m = 1$, and for different values of the Coulomb coupling strength Γ . From figures 4(a) and (b), it is obvious that when the value of the Coulomb coupling strength is weak, the maximum entanglement can be achieve for a low value of temperature and input laser power. In addition, entanglement between the two mechanical resonators decreases when any of the two quantity increase. For strong Coulomb coupling strength as shown in figures 4(c) and (d), we see that for small value of environment temperature, the entanglement first increases, reaches to maximum value and then decrease as we increase the input laser power. Furthermore, one can easily note that the entanglement has a maximum value for a small interval of input laser power. Hence,

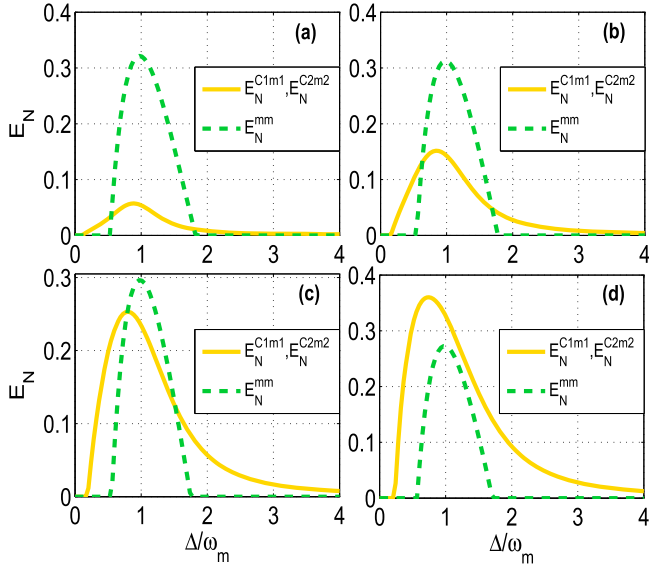


Figure 5. The logarithmic negativity $E_N^{C1m1} = E_N^{C2m2}$ and (dashed green line) E_N^{mm} (solid orange line) as a function of the Δ/ω_m for different values of the input power when (a) $\varphi = 2$ mW, (b) $\varphi = 4$ mW, (c) $\varphi = 6$ mW and (d) $\varphi = 8$ mW. In (a-d), we set $\Gamma = 0.4\omega_m$. The other parameters are same as in figure 2.

we conclude that for strong Coulomb coupling strength, we cannot only enhance but also control the maximum value of the entanglement between mechanical resonators by appropriately adjusting the input laser power. It is interesting to mention here that one can also control as well as enhance the entanglement through optimal control theory [62, 63].

We also investigate the stationary entanglement transfer of the two bipartite subsystems. We denote the logarithmic negativities for mirror 1-mirror 2 and cavity 1-mirror 1/cavity 2-mirror 2 as E_N^{mm} and E_N^{C1m1} ($i = 1, 2$) respectively. As our system is symmetric, so the entanglement between cavity 1-mirror 1 and cavity 2-mirror 2 must be equal i.e. $E_N^{C1m1} = E_N^{C2m2}$. We have studied the entanglement transfer by two ways: firstly, by changing the coupling strength at fixed input power and secondly by changing the input laser power at fixed coupling strength. In figure 5, we have plotted the two bipartite logarithmic negativities E_N^{C1m1} (orange solid line), and E_N^{mm} (green dashed line), versus the normalized detuning Δ/ω_m for fixed value of Coulomb coupling strength. It is obvious that there is a sort of entanglement transfer between two bipartite subsystems, i.e. the bipartite entanglements E_N^{C1m1} increase while the bipartite entanglement E_N^{mm} decrease with the increase of input laser power. In figure 6, we have plotted the two bipartite logarithmic negativities E_N^{C1m1} (orange solid line), and E_N^{mm} (green dashed line), versus the normalized detuning Δ/ω_m for fixed value of input laser power. It can be easily observed that for a fixed value of input laser power, as the Coulomb coupling strength increases, the entanglement between the cavity and mirror increases while the entanglement between the two mechanical resonators decreases. It is obvious that when we increase the input laser power for fixed value of the Coulomb coupling or decrease the Coulomb coupling between the two resonators at fixed value of input laser, the interaction between two resonators

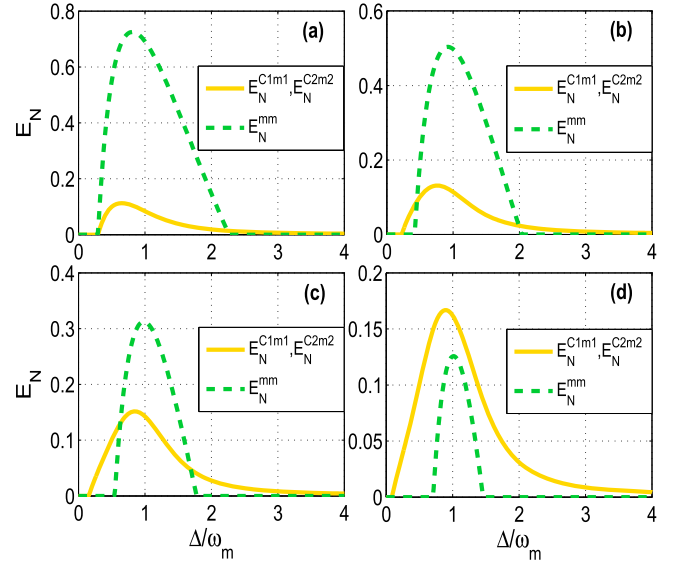


Figure 6. The logarithmic negativity $E_N^{C1m1} = E_N^{C2m2}$ and (dashed green line) E_N^{mm} (solid orange line) as a function of the Δ/ω_m for different values of the coupling strength when (a) $\Gamma = 0.8\omega_m$, (b) $\Gamma = 0.6\omega_m$, (c) $\Gamma = 0.4\omega_m$ and (d) $\Gamma = 0.2\omega_m$. In (a-d), we set $\varphi = 4$ mW. The other parameters are same as in figure 2.

slightly decrease and therefore, entanglement between the mirror-mirror decrease. Hence, it can be clearly seen from the figures 5 and 6 that the bipartite entanglement E_N^{C1m1} is increased while the bipartite entanglement E_N^{mm} is decreased with either by decreasing the coupling strength for a fixed value of input laser field or by increasing the input power from both side for a fixed value of Coulomb coupling strength. In other words, the enhancement of the entanglements E_N^{C1m1} at the expense of the entanglement E_N^{mm} .

In experiments, it is very hard to attain two totally identical mechanical resonators. So, it is very much necessary to discuss the case in which the two separated mechanical resonators in space have unequal frequencies. For this purpose, we plot the logarithmic negativity E_N^{mm} when two mechanical resonators have different frequencies. One can easily observe from figure 7 that the influence of 5% deviation of the frequency of the mechanical resonator on the entanglement between the two mechanical resonators is almost similar. Furthermore, when the frequency of mechanical resonator $\omega_2 = 0.95\omega_1$, the two mechanical resonators are more entangle but the optimal entanglement is shifted towards lower detuning value while if the frequency of mechanical resonator $\omega_2 = 1.05\omega_1$, the entanglement between the two mechanical resonators is slightly reduced and optimal entanglement is moved towards higher detuning value. It is confirmed from the above discussion that small frequency deviation between the two mechanical resonator will not affect the classical to quantum entanglement behavior between the two mechanical resonators separated in space. In addition, the strength of the entanglement can be control by appropriately adjusting the frequencies of the two mechanical resonators.

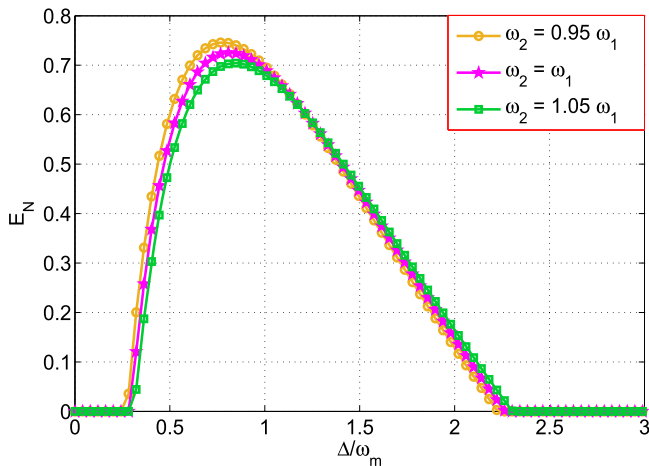


Figure 7. The logarithmic negativity E_N as a function of the Δ/ω_m for identical and different MRs frequencies. The other parameters are same as in figure 2.

5. Conclusion

In conclusion, we have studied the steady state entanglement between the two mechanical resonators which are coupled through Coulomb interaction in coupled optomechanical systems. We have shown that the Coulomb interaction between the mechanical resonators is the essential reason for the existence of entanglement between the two mechanical resonators that are separated in space. Our results show that we can achieve non-zero quantum entanglement between the two mechanical resonators for large Coulomb coupling strengths at small effective temperature even at zero effective optomechanical couplings and show a quantum behavior. Furthermore, an increase in temperature leads to the transition from quantum to classical regime, which is due to the thermal fluctuations which act as a decoherence channel [6]. In addition, the optomechanical coupling strengths of the two cavities are two significant factors to control the entanglement between the two mechanical resonators at different Coulomb coupling strength. Moreover, in experimentally feasible regimes, the results of our numerical simulation showed that we can easily transfer the entanglement, based on our coupled optomechanical system and have shown the transfer of the entanglement from mirror–mirror to the cavity-mirror either by decreasing the Coulomb coupling strength or by increasing the input laser power from both side. Finally, we have shown that we can control and enhance the maximum entanglement through appropriately adjusting the frequencies of the two mechanical resonators. In addition, frequency deviation between the two mechanical resonators cannot affect the classical to quantum transition behavior.

ORCID iDs

Amjad Sohail  <https://orcid.org/0000-0001-8777-7928>
 Chang Shui Yu  <https://orcid.org/0000-0002-8174-3775>

References

- [1] Schrodinger E 1935 *Proc. Camb. Phil. Soc.* **31** 555
- [2] Horodecki R, Horodecki P, Horodecki M and Horodecki K 2009 *Rev. Mod. Phys.* **81** 865
- [3] Giovannetti V, Lloyd S and Maccone L 2011 *Nat. Photon.* **5** 222
- [4] Jones J A and Jaksch D 2012 *Quantum Information, Computation and Communication* (Cambridge: Cambridge University Press) (<https://doi.org/10.1017/CBO9781139028509>)
- [5] Schwab K C and Roukes M L 2005 *Phys. Today* **58** 36
- [6] Zurek W H 1991 *Phys. Today* **44** 36
- [7] Bassi A, Lochan K, Satin S, Singh T P and Ulbricht H 2013 *Rev. Mod. Phys.* **85** 471
- [8] Wang H F, Zhu A D, Zhang S and Yeon K H 2011 *New J. Phys.* **13** 013021
- [9] Sun W M, Su S L, Jin Z, Liang Y, Zhu A D, Wang H F and Zhang S 2015 *J. Opt. Soc. Am. B* **32** 9
- [10] Su S L, Shao X Q, Wang H F and Zhang S 2014 *Phys. Rev. A* **90** 054302
- [11] Su S L, Shao X Q, Wang H F and Zhang S 2014 *Sci. Rep.* **4** 7566
- [12] Su S L, Guo Q, Wang H F and Zhang S 2015 *Phys. Rev. A* **92** 022328
- [13] Wang H F and Zhang S 2009 *Phys. Rev. A* **79** 042336
- [14] Wang H F and Zhang S 2009 *Eur. Phys. J. D* **53** 359
- [15] Wang H F, Zhang S, Zhu A D, Yi X X and Yeon K H 2011 *Opt. Express* **19** 25433
- [16] Cirac J I and Zoller P 1995 *Phys. Rev. Lett.* **74** 4091
- [17] Kielpinski D, Monroe C and Wineland D J 2002 *Nature* **417** 709
- [18] Wilson A C, Colombe Y, Brown K R, Knill E, Leibfried D and Wineland D J 2014 *Nature* **512** 7512
- [19] Monz T et al 2011 *Phys. Rev. Lett.* **106** 130506
- [20] Chen L B, Shi P, Zheng C H and Gu Y J 2012 *Opt. Express* **20** 14547
- [21] Lau H W, Dutton Z, Wang T and Simon C 2014 *Phys. Rev. Lett.* **113** 090401
- [22] Poot M and van der Zant H S J 2012 *Phys. Rep.* **511** 273
- [23] Stannigel K, Komar P, Habraken S J M, Bennett S D, Lukin M D, Zoller P and Rabl P 2012 *Phys. Rev. Lett.* **109** 013603
- [24] Rips S and Hartmann J 2013 *Phys. Rev. Lett.* **110** 120503
- [25] Marquardt F and Girvin S M 2009 *Physics* **2** 40
- [26] Braginsky V and Vyatchanin S P 1999 *Phys. Lett. A* **109** 1–10
- [27] Tetard L, Passian A, Venmar K T, Lynch R M, Voy B H, Shekhawat G, Dravid V P and Thundat T 2008 *Nat. Nanotechnol.* **3** 501
- [28] Zhang J, Peng K and Braunstein S L 2003 *Phys. Rev. A* **68** 013808
- [29] Hartmann M J and Plenio M B 2008 *Phys. Rev. Lett.* **101** 200503
- [30] Liao J Q, Wu Q Q and Nori F 2014 *Phys. Rev. A* **89** 014302
- [31] Pirandola S, Vitali D, Tombesi P and Lloyd S 2006 *Phys. Rev. Lett.* **97** 150403
- [32] Børkje K, Nunnenkamp A and Girvin S M 2011 *Phys. Rev. Lett.* **107** 123601
- [33] Joshi C, Larson J, Jonson M, Andersson E and Öhberg P 2012 *Phys. Rev. A* **85** 033805
- [34] Kimble H J 2008 *Nature* **453** 1023
- [35] Hedemann S R and Clader B D 2018 *J. Opt. Soc. Am.* **35** 2509
- [36] Chen R X, Shen L T and Zheng S B 2015 *Phys. Rev. A* **91** 022326
- [37] Bai C H, Wang D Y, Wang H F, Zhu A D and Zhang S 2017 *Sci. Rep.* **7** 2545
- [38] Bai C H, Wang D Y, Wang H F, Zhu A D and Zhang S 2016 *Sci. Rep.* **6** 33404

- [39] Zhou L, Han Y, Jing J and Zhang W P 2011 *Phys. Rev. A* **83** 052117
- [40] Hartmann M J and Plenio M B 2008 *Phys. Rev. Lett.* **101** 200503
- [41] Low U, Emery V J and Fabricius K 1994 *Phys. Rev. Lett.* **72** 1918
- [42] Bohm D and Pines D 1953 *Phys. Rev.* **92** 609
- [43] Bariani F, Otterbach J, Tan H and Meystre P 2014 *Phys. Rev. A* **89** 011801(R)
- [44] Khazali M 2018 *Phys. Rev. A* **98** 043836
- [45] Ahmed R and Qamar S 2017 *Phys. Scr.* **92** 105101
- [46] Ahmed R and Qamar S 2019 *Phys. Scr.* **94** 085102
- [47] Amjad S, Zhang Y, Usman M and Chang-Shui Y 2017 *Eur. Phys. J. D* **71** 103
- [48] Hensinger W K, Utami D W, Goan H S, Schwab K, Monroe C and Milburn G J 2005 *Phys. Rev. A* **72** 041405(R)
- [49] Ma P C, Zhang J Q, Xiao Y, Feng M and Zhang Z M 2014 *Phys. Rev. A* **90** 043825
- [50] Tian L and Zoller P 2004 *Phys. Rev. Lett.* **93** 266403
- [51] Vitali D *et al* 2007 *Phys. Rev. Lett.* **98** 030405
- [52] Adesso G, Serafini A and Illuminati F 2004 *Phys. Rev. A* **70** 022318
- [53] Vidal G and Werner R F 2002 *Phys. Rev. A* **65** 032314
- [54] Plenio M B 2005 *Phys. Rev. Lett.* **95** 090503
- [55] Gröblacher S, Hammerer K, Vanner M and Aspelmeyer M 2009 *Nature* **460** 724
- [56] Aspelmeyer M and Kippenberg T J 2014 *Rev. Mod. Phys.* **86** 1391
- [57] Meystre P 2013 *Ann. Phys.* **525** 215
- [58] Milburn G J and Woolley M 2011 *Acta Phys. Slovaca* **61** 483
- [59] Aspelmeyer M, Meystre P and Schwab K 2012 *Phys. Today* **65** 29
- [60] Riedinger R *et al* 2018 *Nature* **556** 473
- [61] Marinkovic I *et al* 2018 *Phys. Rev. Lett.* **121** 220404
- [62] Stefanatos D 2017 *Quantum Sci. Technol.* **2** 014003
- [63] Bergholm V, Wieczorek W, Schulte-Herbrüggen T and Keyl M 2019 *Quantum Sci. Technol.* **4** 034001